



Universidade de São Paulo

Biblioteca Digital da Produção Intelectual - BDPI

Departamento de Física e Ciências Materiais - IFSC/FCM

Artigos e Materiais de Revistas Científicas - IFSC/FCM

2010-04

Photodynamic therapy associating Photogem® and blue LED on L929 and MDPC-23 cell culture

Cell Biology International, London : Portland Press, v. 34, n. 4, p. 343-351, Apr. 2010

<http://www.producao.usp.br/handle/BDPI/50178>

Downloaded from: Biblioteca Digital da Produção Intelectual - BDPI, Universidade de São Paulo

Photodynamic therapy associating Photogem[®] and blue LED on L929 and MDPC-23 cell culture

Ana Paula Dias Ribeiro^{*}, Ana Cláudia Pavarina^{1*}, Flávia Zardo Trindade^{*}, Natália Mayumi Inada[†], Vanderlei Salvador Bagnato[†] and Carlos Alberto de Souza Costa[‡]

^{*} Department of Dental Materials and Prosthodontics, São Paulo State University, Araraquara School of Dentistry, Araraquara, SP, Brazil

[†] Physics Institute of São Carlos, University of São Paulo, São Carlos, SP, Brazil

[‡] Department of Physiology and Pathology, São Paulo State University, Araraquara School of Dentistry, Araraquara, SP, Brazil

Abstract

To evaluate the cytotoxicity of PDT (photodynamic therapy) with Photogem[®] associated to blue LED (light-emitting diode) on L929 and MDPC-23 cell cultures, 30000 cells/cm² were seeded in 24-well plates for 48 h, incubated with Photogem[®] (10, 25 or 50 mg/l) and irradiated with an LED source (460 ± 3 nm; 22 mW/cm²) at two energy densities (25.5 or 37.5 J/cm²). Cell metabolism was evaluated by the MTT (methyltetrazolium) assay (Dunnet's post hoc tests) and cell morphology by SEM (scanning electron microscopy). Flow cytometry analysed the type of PDT-induced cell death as well and estimated intracellular production of ROS (reactive oxygen species). There was a statistically significant decrease of mitochondrial activity (90% to 97%) for all Photogem[®] concentrations associated to blue LED, regardless of irradiation time. It was also demonstrated that the mitochondrial activity was not recovered after 12 or 24 h, characterizing irreversible cell damage. PDT-treated cells presented an altered morphology with ill-defined limits. In both cell lines, there was a predominance of necrotic cell death and the presence of Photogem[®] or irradiation increased the intracellular levels of ROS. PDT caused severe toxic effects in normal cell culture, characterized by the reduction of the mitochondrial activity, morphological alterations and induction of necrotic cell death.

Keywords: cytotoxicity; fibroblast; haematoporphyrin derivative; odontoblast; photodynamic therapy

1. Introduction

PDT (photodynamic therapy) has been widely used in different dental areas over the last decades, and excellent results have been reported after its application for the treatment of oral cancer and premalignant lesions (Allison et al., 2005, 2006; Yu et al., 2008) as well as bacterial and fungal infections (Teichert et al., 2002; Williams et al., 2006; Donnelly et al., 2007). The simplicity of the PDT mechanism stimulated interest in this therapy, which is characterized by the association of a photosensitizing agent and visible light with a wavelength compatible with the photosensitizer's absorption spectrum (Konopka and Goslinski, 2007; Buytaert et al., 2007). Photon absorption by the photosensitizer leads it to a triple state of excitation that may interact with the available oxygen, producing ROS (reactive oxygen species) and singlet oxygen (Wainwright, 1998). All these products, originating from PDT, may result in a cascade of oxidative events that cause direct cell death, destruction of tumour vascularization and activation of the host's immune response (Wainwright, 1998).

Antimicrobial PDT has been indicated as an alternative treatment for the elimination of microorganisms, especially pathogens that are refractory to conventional therapies. The singlet oxygen and all other released free radicals interact by different mechanisms with diverse microbial cell structures, such as proteins, lipid membranes and nucleic acids, resulting in apoptotic or necrotic cell death (Konopka and Goslinski, 2007). The

increase of fungal infection incidence has been attributed to indiscriminate use of broad-spectrum antibiotics, antifungal agents and immunosuppressive drugs (Donnelly et al., 2008). Additionally, there is a high incidence of *Candida* ssp. infections in immunodepressed and aged patients who continuously wear removable dentures (Nikawa et al., 2003; Donnelly et al., 2008). Since the oral cavity has an easy access for irradiation and application of drugs with photosensitizing properties, PDT has been indicated for the treatment of denture-induced stomatitis (Donnelly et al., 2008), which is characterized as a clinical manifestation of oral candidosis related to the use of complete dentures (Chandra et al., 2001).

Inactivation of *Candida* strains has been demonstrated in several studies (Wilson and Mia, 1993; Zeina et al., 2001; Teichert et al., 2002; Lambrechts et al., 2005a; Donnelly et al., 2007). However, it has been reported that this fungus is more resistant and refractory to treatment than Gram-positive bacteria (Lambrechts et al., 2005a). According to Demidova and Hamblin (2005), the nuclear membrane, the larger size of the fungal cell and the lower number of targets for the singlet oxygen per cell unit volume, require a greater concentration of photosensitizer and a greater amount of light to inactivate the yeast. In addition, the similarity between fungal cells and the mammalian cells hinders the selective accumulation of the photosensitizer in the yeast (Donnelly et al., 2008).

Therefore, in order to consider the antifungal PDT as a clinical treatment for denture-induced stomatitis, it is necessary to know its antifungal potential, as well as its cytotoxic effect on the

¹ To whom correspondence should be addressed (email pavarina@foar.unesp.br).

Abbreviations: DCF, dichlorodihydrofluorescein; DMEM, Dulbecco's modified Eagles medium; H₂-DCFDA, 2',7'-dichlorodihydrofluorescein diacetate; LED, light-emitting diode; MTT, 3-(4,5-dimethylthiazol-2-yl)-2,5-diphenyl-2H-tetrazolium bromide; PDT, photodynamic therapy; ROS, reactive oxygen species; SEM, scanning electron microscopy.

individual's normal cells. The effect of PDT with some photosensitizers on keratinocyte and fibroblast cultures has been demonstrated by several *in vitro* studies (Zeina et al., 2002; Zeina et al., 2003; Chiu et al., 2005; Lambrechts et al., 2005b). However, the toxicity of Photogem[®], a first-generation haematoporphyrin-derived photosensitizer, associated with LEDs (light-emitting diodes) on the normal cells has not yet been described. LED systems are still not widely used in PDT and have been suggested as a substitute to laser and optic fibers because they are easy to handle, portable, cost-effective and available in a variety of shapes and sizes (Konopka and Goslinski, 2007). Therefore, this study evaluated the *in vitro* cytotoxicity of the antifungal PDT with the photosensitizer Photogem[®] associated to blue LED on fibroblast L929 and odontoblast-like MDPC-23 cell cultures. For such purposes, cell metabolism was evaluated by the MTT [3-(4,5-dimethylthiazol-2-yl)-2,5-diphenyl-2H-tetrazolium bromide] assay 0, 12 and 24 h after PDT. Cell morphology was analysed by SEM (scanning electron microscopy). Flow cytometry was employed to analyse the type of PDT-induced cell death (necrosis or apoptosis) using annexin V and propidium iodine staining as well as to estimate the intracellular levels of ROS using H₂-DCFDA (2',7'-dichlorodihydrofluorescein diacetate) staining.

2. Materials and methods

2.1. Photosensitizer and light source (blue LED)

Photogem[®] is a first-generation haematoporphyrin-derived photosensitizer (Limited Liability Company). The clinical application of this photosensitizing agent in humans has been allowed by the State Pharmacological Committee of the Russian Federation, where the product has been developed. In Brazil, the clinical use of Photogem[®] has been approved by the ANVISA (Brazilian National Health Surveillance Agency). A stock solution of the photosensitizer Photogem[®] was prepared in serum-free DMEM (Dulbecco's modified Eagle's medium) without Phenol Red (Sigma Chemical) at a concentration of 1000 mg/l and stored at 4°C. The Photogem[®] concentrations used in the present study (10, 25 and 50 mg/l) were obtained by dilution of the stock solution.

An LED system with a predominant wavelength of 455 nm developed by the Physics Institute of São Carlos (University of São Paulo, São Carlos, SP, Brazil) was used to excite the photosensitizer. This system, called Biotable, is composed of eight royal blue LEDs (LXHL-PR09 Luxeon[®] III Emitter, Lumileds Lighting) that are uniformly distributed into the device. This distribution allowed a homogenous illumination of the surface of a 24-well plate (Costar Corp.) with a light intensity of 22 mW/cm². The cells were submitted to two energy densities, 25.5 and 37.5 J/cm², according to an exposure time to the blue LED of 19 and 28 min respectively.

2.2. Cell culture

The two cell lines used in this study were immortalized L929 fibroblasts, purchased from Adolfo Lutz Institute, and immortalized odontoblast cell line MDPC-23, cultured at the Laboratory of

Experimental Pathology and Biomaterials of Araraquara Dental School, Brazil (Hanks et al., 1998). Both cell lines were cultured in DMEM (Sigma Chemical) supplemented with 10% bovine fetal serum (Gibco), with 100 units/ml penicillin, 100 µg/ml streptomycin and 2 mmol/l glutamine (Gibco) in a humidified incubator with 5% CO₂ and 95% air at 37°C (Isotemp Fisher Scientific). The cells were subcultured every 3 days until an adequate number of cells were obtained for the study. After reaching approximately 80% density, the cells were trypsinized, seeded in sterile 24-well plates (30 000 cells/cm²) and incubated for 48 h.

2.3. PDT

After 48 h of incubation, the culture medium was removed, and cells were washed with PBS. The following groups were formed, according to the treatment received: PDT (Photogem[®] 10, 25 or 50 mg/l+blue LED 25.5 or 37.5 J/cm²); Photogem[®] (10, 25 or 50 mg/l); blue LED (25.5 or 37.5 J/cm²) and negative control (no treatment). The experimental and control groups are summarized in Table 1. Aliquots of 1 ml of Photogem[®] at each concentration (10, 25 or 50 mg/l) or DMEM without Phenol Red were transferred individually to wells of 24-well plates and were incubated in contact with the cells for 30 min protected from light. After the incubation period, PDT and blue LED groups were irradiated using the Biotable system for 19 or 28 min corresponding to energy densities of 25.5 or 37.5 J/cm², respectively. The Photogem[®] group and the negative control group were maintained under dark conditions for the same period corresponding to irradiation (19 or 28 min).

2.4. Analysis of cell metabolism (MTT assay)

Cell metabolism was evaluated by SDH (succinic dehydrogenase) enzyme, which is a measure of the mitochondrial respiration of the cell (Mosmann, 1983). For this purpose, the MTT assay was used, and mitochondrial activity was assessed 0, 12 and 24 h after PDT. In 10 wells, 900 µl of DMEM in addition to 100 µl of MTT solution (5 mg/ml sterile PBS) (Sigma Chemical) was applied to the cells cultured in each well and incubated at 37°C for 4 h. Thereafter, the culture medium (DMEM with the MTT solution) was aspirated and replaced by 600 µl of acidified propan-2-ol solution (0.04 M HCl) to dissolve the blue crystals of formazan present in the cells.

Table 1 Experimental groups and treatments
P, Photogem[®]; L, light.

Groups	Treatment
Negative control (no treatment)	P-L-
Photogem [®]	P+10 L-
	P+25 L-
	P+50L-
Blue LED	P-L+ (19 min)
	P-L+ (28 min)
PDT	P+10L+ (19 min)
	P+25L+ (19 min)
	P+50L+ (19 min)
	P+10L+ (28 min)
	P+25L+ (28 min)
	P+50L+ (28 min)

Cell metabolism was determined as being proportional to the absorbance measured at 570 nm wavelength with an ELISA plate reader (Bio-Rad, model 3550-UV, microplate reader). The MTT assay data presented a normal distribution and was analysed statistically by ANOVA and Dunnet's post hoc tests.

2.5. Analysis of cell morphology by SEM

For cell morphology analysis by SEM, sterile 12-mm-diameter cover glasses (Fisher Scientific) were placed at the bottom of the wells of all experimental and control groups immediately before seeding the cell lines. After the experimental conditions had been applied, the culture medium was removed, and the viable cells that remained adhered to the glass substrate were fixed in 1 ml of buffered 2.5% glutaraldehyde for 24 h and postfixed with 1% osmium tetroxide for 1 h. The cells adhered to the glass substrate were then dehydrated in a series of increasing ethanol concentrations (30%, 50%, 70%, 95% and 100%) and immersed in HMDS (1,1,1,3,3,3-hexamethyldisilazane; Acros Organics) for 90 min [23] and stored in a desiccator for 24 h. The coverglasses were then mounted on metallic stubs, sputter-coated with gold, and the morphology of the surface-adhered L929 and MDPC-23 cells were examined with a scanning electron microscope (JEOL-JMS-T33A Scanning Microscope).

2.6. Type of cell death (annexin-V and propidium iodide assay)

Both cell lines (L929 and MDPC-23) were cultured as monolayers in 75-cm² cell culture flasks, and after reaching approximately 80% density, the cells were trypsinized and seeded in 25-cm² cell culture flasks (30 000 cell/cm²). After 72 h in a humidified incubator, the culture medium was removed, and the cells were exposed to Photogem[®] at experimental concentrations (10, 25 or 50 mg/l) or to DMEM without Phenol Red for 30 min. Then, groups PDT and blue LED were irradiated for 28 min (37.5 J/cm²). After these procedures, the cells were trypsinized and centrifuged at 500 rev./min for 5 min. The supernatant was discarded, and the cells were resuspended in 1 ml of ligation buffer containing 10 mM Hepes pH 7.4, 150 mM NaCl, 5 mM KCl, 1 mM MgCl₂ and 1.8 mM CaCl₂. The cells were stained and analysed by FACS in a flow cytometer (FACSCalibur; BD Biosciences) equipped with argon laser and CellQuest software (BD Biosciences). At least 10 000 events were collected for each sample. For acquisition of the cells labelled positively for apoptosis, an aliquot of 250 µl of cell suspension of each experimental condition and the negative control were treated with annexin-V (Biomedical Sciences Institute) at a concentration of 1:500 for 20 min in the dark. The apoptotic cells were acquired in the FL-1 channel of the flow cytometer. The cells labelled positively for necrosis were acquired immediately after the addition of 0.2 µg/ml of propidium iodide in the FL-2 channel of the flow cytometer.

2.7. Analysis of intracellular ROS

Under the same conditions described for detection of the type of cell death, cellular ROS production was monitored by

spectrofluorimetry using a membrane-permeable fluorescent probe, H₂-DCFDA (Invitrogen), which is more specific for the detection of H₂O₂ (hydrogen peroxide). After cell resuspension in ligation buffer, an aliquot of 250 µl of cell suspension of each experimental condition and negative control was treated with H₂-DCFDA 1 µM for 20 min in the dark. In the presence of ROS, the H₂-DCFDA is oxidated and converted into DCF (dichlorodihydrofluorescein), which emits fluorescence at 525 nm upon excitation at 488 nm by the flow cytometer. The calibration was made by the addition of known concentrations of DCF. DCF fluorescence was monitored in the FL-1 of the flow cytometer. Data referring to the type of cell death and intracellular ROS production were analysed by paired Student's *t* test. All statistical analyses were done at the 5% significance level and using SYSTAT software 5.03 for Windows (SYSTAT, Inc.).

3. Results

3.1. Cell metabolism (MTT assay)

Figures 1, 2, 3 and 4 present the effect of PDT (P+L+), different Photogem[®] concentrations (P+L-) and the blue LED (P-L+) at the different periods of cell metabolism evaluation (0, 12 and 24 h). Considering the negative control group (P-L-) as having 100% of L929 and MDPC-23 cell metabolism, a significant reduction of cell metabolism (from 90% to 97%; *P*<0.05) was observed for all Photogem[®] concentrations when the cells were irradiated by the blue LED at both energy densities (25.5 and 37.5 J/cm²). In those groups, there was no statistically significant difference (*P*>0.05) among the Photogem[®] concentrations (10, 25 and 50 mg/l).

The toxicity of Photogem[®] without exposure to light was also evaluated. An initial stimulation of the mitochondrial activity (0 h) was observed, which returned to normality within 24 h. Regarding the effect of light, only the groups exposed to blue LED for 28 min (37.5 J/cm²) had their mitochondrial activity reduced 24 h after irradiation. Compared with the negative control, the metabolism of

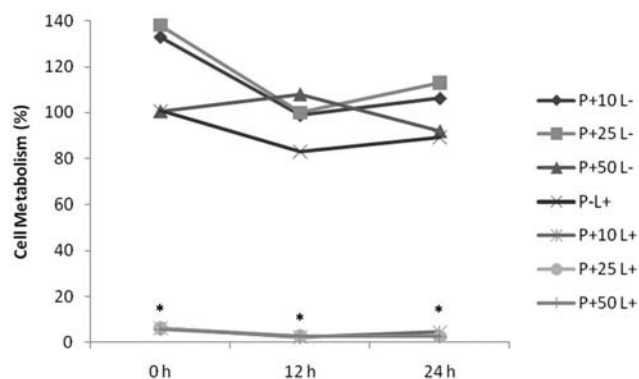


Figure 1 Graphic presentation of the percentage values of fibroblast L929 cell line metabolism over time (0, 12 and 24 h) considering the negative control (P-L-) as 100%

The irradiation dose was 25.5 J/cm² (19 min) for groups P-L+ and P+L+. The asterisks indicate values that were significantly different from 100% (Dunnet's post hoc, *P*<0.05). Each point represents the average of 10 values (*n*=10).

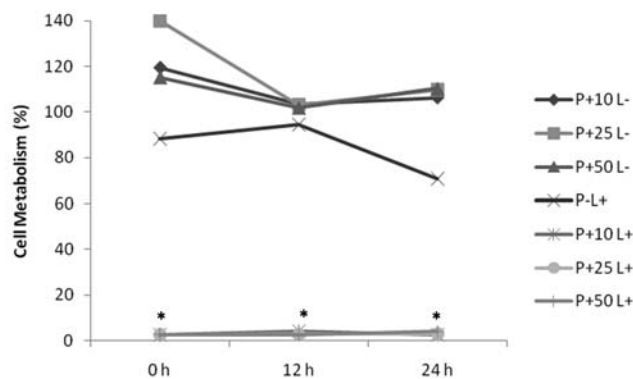


Figure 2 Graphic presentation of the percentage values of fibroblast L929 cell line metabolism over time (0, 12 and 24 h) considering the negative control (P-L-) as 100%

The irradiation dose was 37.5 J/cm^2 (28 min) for groups P-L+ and P+L+. The asterisks indicate values that were significantly different from 100% (Dunnet's post hoc, $P < 0.05$). Each point represents the average of 10 values ($n=10$).

L929 fibroblasts and MDPC-23 cells decreased by 30% (Figure 2) and 23% (Figure 4), respectively.

3.2. Cell morphology (SEM)

Figure 5(a)–5(f) presents a panel of SEM micrographs of the L929 fibroblasts representative of the experimental and control groups. For the negative control group (no treatment) and the groups treated with blue LED or Photogem® (50 mg/l) alone, numerous L929 fibroblasts that remained adhered to the glass substrate exhibited a spindle-shaped appearance with few cytoplasmic processes originating from the membrane (Figures 5a, 5e and 5f). However, the negative control group exhibited a larger number of mitoses when compared with the blue LED and Photogem® controls. In the groups submitted to PDT, there was a smaller number of L929 fibroblasts that remained adhered to the cover-glass. These cells were round-shaped and small-sized and exhibited fine and sometimes fragmented cytoplasmic processes.

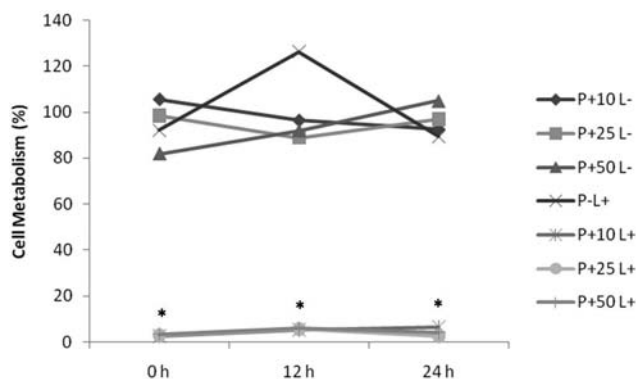


Figure 3 Graphic presentation of the percentage values of MDPC-23 odontoblast-like cell line metabolism over time (0, 12 and 24 h) considering the negative control (P-L-) as 100%

The irradiation dose was 25.5 J/cm^2 (19 min) for groups P-L+ and P+L+. The asterisks indicate values that were significantly different from 100% (Dunnet's post hoc, $P < 0.05$). Each point represents the average of 10 values ($n=10$).

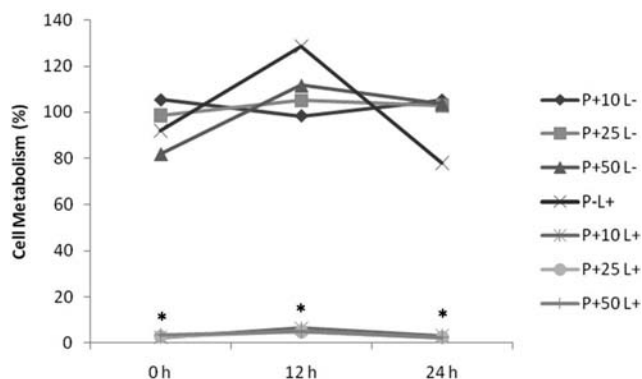


Figure 4 Graphic presentation of the percentage values of MDPC-23 odontoblast-like cell line metabolism over time (0, 12 and 24 h) considering the negative control (P-L-) as 100%

The irradiation dose was 37.5 J/cm^2 (28 min) for groups P-L+ and P+L+. The asterisks indicate values that were significantly different from 100% (Dunnet's post hoc, $P < 0.05$). Each point represents the average of 10 values ($n=10$).

In some areas of the glass substrate, remnants of cytoplasmic membrane of dead cells were observed (Figures 5b, 5c and 5d). This altered morphology observed immediately after PDT (0 h) remained unchanged within the following 24 h, demonstrating the irreversible nature of the damage caused by the PDT (Figure 5d).

Figures 6(a)–6(f) presents a panel of SEM micrographs of the MDPC-23 odontoblast-like cells. These cells exhibited a wide cytoplasm and numerous fine cytoplasmic processes originating from the cell membrane (Figures 6a, 6e and 6f). The blue LED group irradiated with an energy density of 37.5 J/cm^2 presented similar morphology to that of the negative control group. On the other hand, the Photogem® (50 mg/l) group presented a smaller number of cells adhered to the glass substrate and some cell-free regions, compared with the negative control group (Figure 6e). The groups submitted to the PDT presented an intense alteration of the cell morphology, and it was not possible to identify the cell cytoplasmic membrane. The few cells that remained adhered to the glass substrate were small-sized and round-shaped (Figures 6b, 6c and 6d). This altered morphology observed immediately after PDT (0 h) remained unchanged within the following 24 h, demonstrating the irreversible nature of the damage caused by the PDT (Figure 6d).

3.3. Cell death induced by PDT

The type of cell death (apoptosis and necrosis) for both cell lines (L929 e MDPC-23) caused by the contact with the Photogem® associated or not to blue LED irradiation was evaluated by flow cytometry. The exposure of MDPC cells to the three concentrations of the photosensitizer (10, 25 and 50 mg/l) in the absence of light induced 0.42%, 1.14% and 1.51% of apoptotic cell death, respectively, and 1.14%, 13.85% and 34.69% necrotic cell death respectively (Figure 7). The exposure of the L929 fibroblasts to the three concentrations of the photosensitizer (10, 25 and 50 mg/l) in the absence of light induced 2.59%, 1.33% and 0.79% of apoptotic cell death respectively and 6.59%, 7.85%, and 9.13% of necrotic cell death respectively (Figure 7). These results indicate

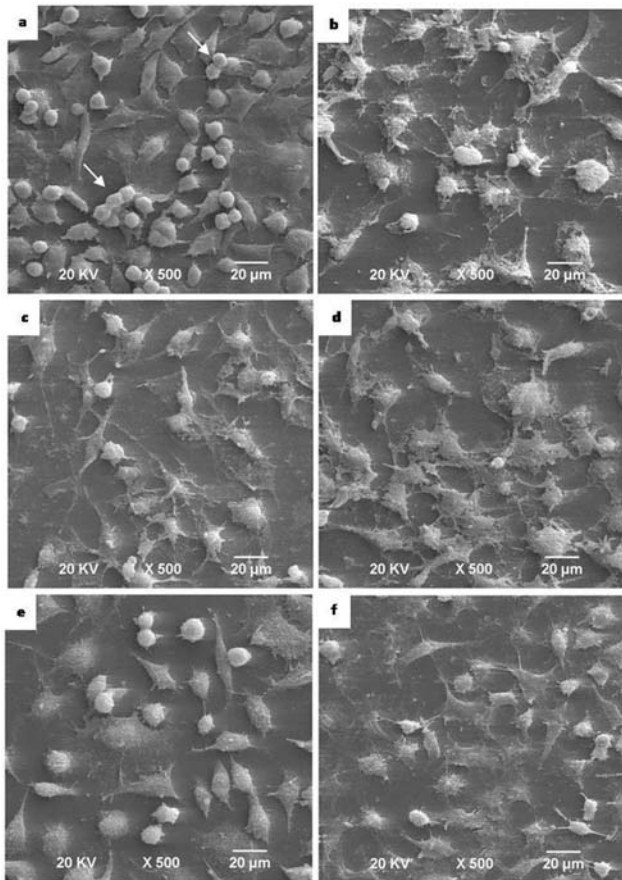


Figure 5 SEM micrographs of the L929 cell line

(a) Negative control group of L929 fibroblasts: a large number of L929 fibroblasts can be observed and numerous mitoses are occurring (arrows). These cells are spindle-shaped cells present as fine cytoplasmic processes covering the glass substrate. SEM, $\times 500$. (b) Group PDT/Photogem[®] (10 mg/l) irradiated for 28 min: fibroblasts exhibit an altered morphology with ill-defined cell limits. The cells are small-sized, and cell remnants can be observed adhered to the glass substrate. SEM, $\times 500$. (c) Group PDT/Photogem[®] (50 mg/l) irradiated for 28 min: the cells present the same characteristics as those of the cells treated with 10 mg/l concentration (Figure 5b), indicating the lack of differences between the Photogem[®] concentrations in this cell line. SEM, $\times 500$. (d) Group PDT/Photogem[®] (50 mg/l) irradiated for 28 min: there was maintenance of the morphological alterations of the L929 fibroblasts 24 h after PDT, demonstrating the irreversible damage cause by this therapy. SEM, $\times 500$. (e) Group Photogem[®] (50 mg/l): The L929 fibroblasts did not exhibit morphological alterations after contact with the Photogem[®] even at the highest concentration evaluated. However, there was a smaller number of cells adhered to the glass substrate and a smaller number of mitoses. SEM, $\times 500$. (f) Group light: the cells of this group were irradiated with the highest energy density (37.5 J/cm^2). There were no significant morphological alterations, although a smaller number of cells remained adhered to glass substrate compared with the control group. SEM, $\times 500$.

a predominance of necrotic cell death for both cell lines under these conditions. For PDT groups (Photogem[®]+blue LED), the destruction of both cell lines was so intense that it was not possible to identify and acquire the cells labelled positively for either apoptosis or necrosis by flow cytometry, making this technique unviable for analysis of the type of cell death in these groups.

3.4. Intracellular ROS production

In the negative control group, intracellular ROS production by both cell lines (L929 and MDPC-23) was negligible. The contact with

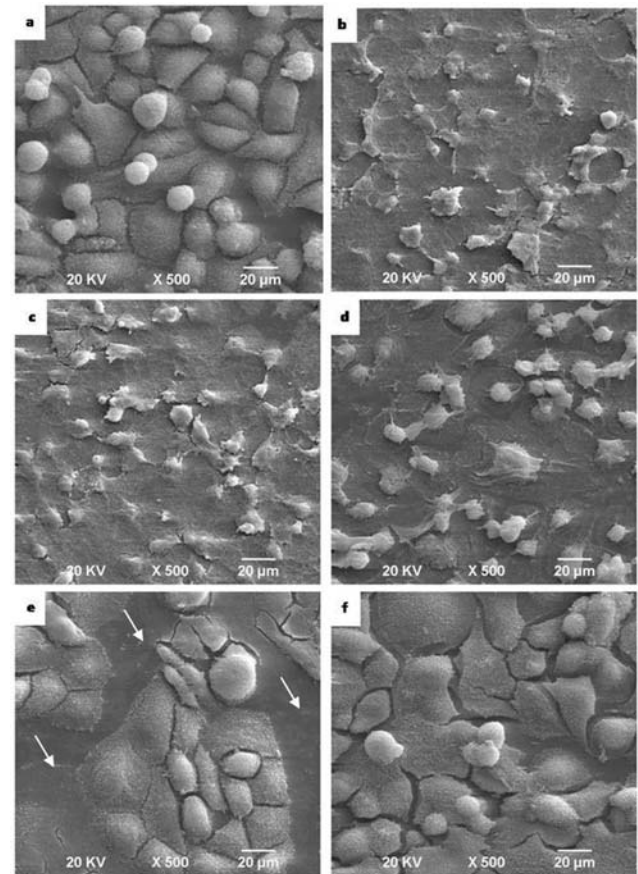


Figure 6 SEM micrographs of the MDPC-23 cell line

(a) Negative control group of odontoblast-like cells: a large number of MDPC-23 cells can be observed adhered to the glass substrate. These cells present a wide cytoplasm and multiple cytoplasmic processes that seem to be keeping the cells attached to the glass substrate. SEM, $\times 500$. (b) Group PDT/Photogem[®] (10 mg/l) irradiated for 28 min: the MDPC-23 cells exhibit an altered morphology with ill-defined limits. The cells are small-sized, and cell remnants can be observed adhered to the glass substrate. SEM, $\times 500$. (c) Group PDT/Photogem[®] (50 mg/l) irradiated for 28 min: the cells present the same characteristics as those of the cells treated with 10 mg/l concentration (Figure 6b), indicating the lack of differences between the Photogem[®] concentrations in this cell line. (d) Group PDT/Photogem[®] (50 mg/l) irradiated for 28 min: there was maintenance of the morphological alterations of the MDPC-23 L929 fibroblasts 24 h after PDT, demonstrating the irreversible damage cause by this therapy. SEM, $\times 500$. (e) Group Photogem[®] (50 mg/l): The MDPC-23 cells did not exhibit morphological alterations after contact with the Photogem[®] even at the highest concentration evaluated. However, some cell-free areas could be also seen (arrows). SEM, $\times 500$. (f) Group light: the cells of this group were irradiated with the highest energy density (37.5 J/cm^2). There were no morphological alterations compared with the control. SEM, $\times 500$.

Photogem[®] without light activation increased significantly intracellular ROS production in a dose-dependent manner in all experimental groups compared with negative control ($P < 0.05$). However, there was no statistically significant difference among the photosensitizer concentrations (10, 25 and 50 mg/l) on the same cell line. The MDPC-23 cell line presented higher intracellular ROS levels compared with L929 fibroblasts. The irradiation of both cell lines for 28 min (37.5 J/cm^2) in the absence of photosensitizer also produced high intracellular ROS levels ($P < 0.05$). The level of ROS revealed a fluorescence intensity value which is presented in Figure 8. Again, for PDT groups

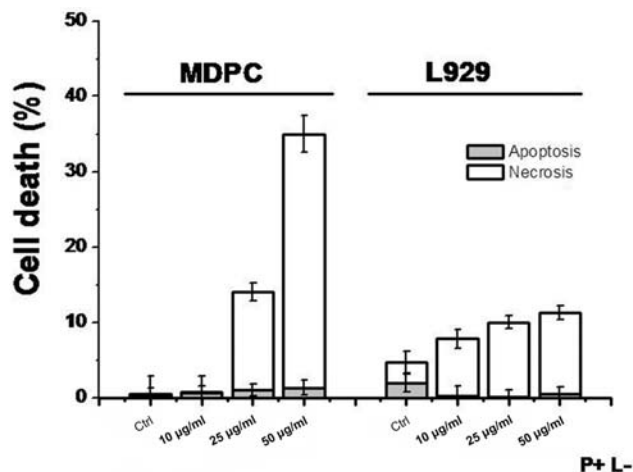


Figure 7 Graphic presentation of the percentage of Photogem[®]-induced cell death

The L929 and MDPC-23 cells were incubated with the different Photogem[®] concentrations (10, 25 and 50 mg/l), and the type of cell death was evaluated by flow cytometry with annexin-V and propidium iodide staining. Ctrl, control.

(Photogem[®]+blue LED), the destruction of both cell lines was so intense that it was not possible to acquire the cells labelled stained with H₂-DCFDA by flow cytometry, making this technique unviable for analysis of the intracellular ROS production in these groups.

4. Discussion

The present study evaluated the cytotoxic potential of PDT with Photogem[®] associated to a blue LED system on L929 fibroblast and odontoblast-like MDPC-23 cell cultures. These cell lines have been widely used to evaluate the *in vitro* cytotoxic effects of biomaterials and dental materials (Serrano et al., 2005; Aranha et al., 2006; Jorge et al., 2007; de Souza Costa et al., 2008). The use of more than one type of cell culture has been suggested by some

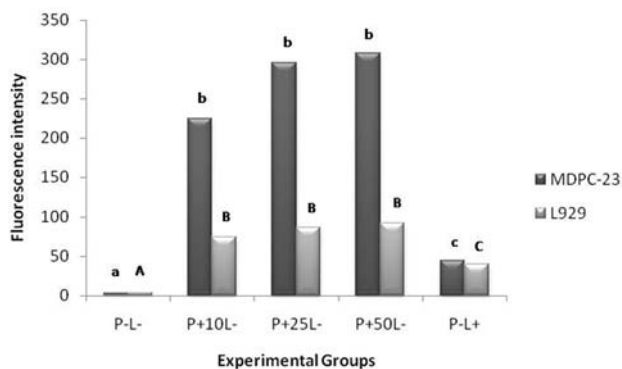


Figure 8 ROS produced by the contact of Photogem[®] and blue light irradiation on L929 and MDPC-23 cells monitored by DCFDA fluorescence detected by flow cytometry

Bars with the same letters represent means of four independent experiments that do not differ significantly (Student's *t* test; $P > 0.05$).

authors due to the different cell responses observed after PDT, and the effects of this therapy are considered to be cell-dependent (Ahn et al., 2004; Postigo et al., 2006). However, in the present study, both the L929 fibroblasts and the odontoblast-like MDPC-23 cells presented similar responses in the MTT assay, and both had their morphology considerably altered by PDT, showing disruption of cell membrane. However, in the cell death and ROS production assays, MDPC-23 showed high levels of necrotic death and ROS production possibly due to its potential to accumulate Photogem[®] and further generating high levels of singlet oxygen and hydrogen peroxide.

The clinical relevance of this study is to investigate whether parameters used for inactivation of fungal species by PDT could result in cytotoxic effects to the host's normal cells. Zeina et al. (2001) reported that the minimum PDT time needed for causing irreversible damage on keratinocytes was 200-fold longer than that required for inactivating bacteria. However, the minimum PDT time was only 18-fold longer than that required for inactivation of *Candida albicans*. These results suggest that PDT was able to inactivate both bacteria and *C. albicans* without causing damage to the normal cells and that inactivation of the yeast required a longer irradiation time. Lambrechts et al. (2005b) evaluated the cytotoxic effects of antifungal PDT on fibroblasts. These authors observed total reduction of cell metabolism when TriP[4] porphyrin was used at doses over 12.5 µM and that the inactivation dose for *C. albicans* was 25 µM. In the present study, the results of the MTT assay revealed a high toxicity of PDT to both cell lines. The association of all Photogem[®] concentrations (10, 25 and 50 mg/l) with both blue LED energy densities (25.5 and 37.5 J/cm²) reduced significantly the cell metabolism (Figures 1–4). The parameters used in this study were previously established based on data obtained in our laboratory referring to specific PDT parameters for inactivation of standard and fluconazol resistant *C. albicans* and *Candida glabrata* strains. Inactivation of *Candida* ssp. by PDT is a complex and multistaged process, different from the inactivation of bacteria, which is a simpler process. However, as PDT effectiveness depends on ROS and singlet oxygen generation, a greater quantity of these compounds must be produced to act on larger-sized cells that present a greater variety of targets, including an additional barrier like the nuclear membrane (Demidova and Hamblin, 2005). Therefore the inactivation of the different *Candida* species requires a higher photosensitizer concentration and a higher energy density, which increases the probability of causing damage to the host's normal cells (Lambrechts et al., 2005a).

There are a number of factors related to PDT toxicity, such as the type of photosensitizer, light intensity, cell type and preincubation time with the drug (Hsieh et al., 2003). In the present *in vitro* study, no direct relationship was observed between the increase in the photosensitizer concentration and the damage caused to the L929 and MDPC-23 cells. The lowest photosensitizer concentration (10 mg/l) was as toxic as the highest concentration (50 mg/l), regardless of the blue LED irradiation time. This result differs from those previous studies, which reported a dose-dependent relationship between the photosensitizer concentration and PDT toxicity for microorganisms or malignant cells (Ahn et al., 2004; Bliss et al., 2004; Demidova and Hamblin, 2005). Some studies

(Maisch et al., 2005; Bouillaguet et al., 2008) have found that the dependence between drug concentration and cell damage was generally in evidence when decimal dilutions (10^1 , 10^2 , 10^3) of photosensitizer were used, which did not occur in this study. In addition, the data obtained in the present study suggest that the cell preincubation time with Photogem® (30 min) was able to sensitize and saturate the cell sites in both L929 fibroblasts and odontoblast-like cells, even when the lowest photosensitizer concentration was used. The analysis by flow cytometry revealed that the intracellular ROS levels produced by the L929 fibroblasts and MDPC-23 cells after blue LED irradiation were able to cause equally irreversible cell damage for the three photosensitizer concentrations (10, 25 or 50 mg/l) (Figure 8). It was also observed that contact with the Photogem® increased the ROS levels for the three photosensitizer concentrations compared with the negative control, in such a way that the ROS levels produced after cell contact with the 10 mg/l concentration did not differ significantly from those obtained with the 50 mg/l concentration.

The irreversibility of the cell damage caused by the PDT was demonstrated by the evaluation of cell metabolism at different periods after treatment (0, 12 and 24 h). The results revealed that even 24 h after PDT, cell metabolism remained between 3% and 10% compared with the negative control group (no treatment), which was considered as having 100% of metabolism. The evaluation of mitochondrial activity over time is recommended because it has been demonstrated that the MTT assay performed immediately after PDT provides higher cell metabolism values compared with those obtained after longer evaluation periods (Lambrechts et al., 2005b; Postigo et al., 2006). This result suggests a continuous and cumulative effect of the light-activated photosensitizer on cell culture. In this study, the cytotoxic effects of the PDT persisted with time, which indicates that both L929 fibroblasts and MDPC-23 cells were unable to recover within 24 h after PDT application. The SEM micrographs confirmed that the damage caused by the PDT were irreversible (Figures 5d and 6d) since the cells maintained the same morphological alterations 24 h after the PDT. In the groups subjected to PDT, there was severe cell destruction, with altered morphology, smaller size and smaller number of cells adhered to the coverglass. In addition, there were cell fragments and ill-defined cytoplasmic membrane limits in the cells subjected to PDT (Figures 5 and 6).

Ahn et al. (2004) evaluated the antitumour effect of the PDT using Photogem® on four uterine cancer cell lines. The authors observed that cell irradiation in the presence of Photogem® induced plasma membrane disruption and cell shrinkage, indicating the plasma membrane as the main target for this photosensitizer. As a rule, photosensitizer accumulation in the mitochondria or endoplasmic reticulum causes apoptosis, while its accumulation in the plasma membrane or lysosomes predisposes the cells to necrosis (Buytaert et al., 2007). In order to characterize the type of cell death resulting from the PDT with Photogem®, annexin-V and propidium iodine staining were used to label the cells positively for apoptosis and necrosis, respectively. However, the cell damage observed after PDT was so severe that the flow cytometry was unable to identify and label either of the cell lines (L929 and MDPC-23). Analysis of the type of cell death by flow cytometry was successful only for the groups

exposed to the photosensitizer without light association (P+L-). For the MDPC-23 cells, it was observed that the higher the photosensitizer concentration (50 mg/l) the larger the number of dead cells, estimated as 34.69% of necrotic cell death (Figure 7). This cell line was more sensitive to the contact with Photogem® compared with the L929 fibroblasts, which exhibited the highest necrotic cell death rate (9.13%) with the 25 mg/l concentration (Figure 7).

The isolated effect of light on the L929 and MDPC-23 cell cultures was also observed in the present study because it is known that the light may have either a stimulating or an inhibitory effect on cell metabolism (Karu, 1990). At 24 h, a reduction of cell metabolism was observed for the cells irradiated for 28 min (37.5 J/cm^2), although not statistically significant. Reduction of cell metabolism after exposure to visible light has been reported in previous studies (Wataha et al., 2004; Taoufik et al., 2008). Zeina et al. (2002) observed that the longer the exposure time, the more severe the cell damage and lesser the cell recovery after PDT. High light intensities have been described to lead to the formation of intracellular ROS, which may interact with endogenous photosensitizers such as flavines and cytochrome *c*, causing cell damage or even death (Karu, 1990). Lockwood et al. (2005) observed that an energy density of 30 J/cm^2 produced high ROS levels and that the presence of antioxidants was shown to reduce the toxic effects to the cells, thereby confirming that the ROS are responsible for the reduction of cell metabolism. In the present study, the intracellular ROS levels were also evaluated for L929 and MDPC-23 cells exposed to the blue LED without photosensitizer, and greater ROS formation in the irradiated groups could be observed compared with the negative control group ($P < 0.05$). Therefore, the data suggest that ROS produced by the irradiated cells might have caused the cell damage observed 24 h after the treatment (Figure 8).

Although the results of the present study demonstrate a cytotoxic effect of PDT on the normal cell cultures, the importance of developing alternative treatments for microbial control, especially those resistant to conventional treatments is recognized. The antimicrobial effect of haematoporphyrin derivatives has been widely studied, and their effectiveness has been confirmed by several studies (Bertoloni et al., 1989; Bliss et al., 2004; Lambrechts et al., 2005a). However, since PDT efficacy depends on the combination of a number of factors, the major challenge for this therapy is to develop a single protocol that is able to inactivate different microbial species without harming the host's normal cells. Further *in vitro* and *in vivo* studies are required to develop PDT protocols that could inactivate *Candida* strains without harming the host's normal tissues and contribute to the treatment of oral candidosis.

5. Conclusions

The results of this study suggest that the PDT with Photogem® associated to blue LED using the parameters established for inactivation of *Candida* ssp. presented severe toxicity to L929 fibroblasts and odontoblast-like MDPC-23 cell cultures. There was a marked decrease of cell metabolism mostly due to necrotic

cell death, characterized by damage to the cytoplasmic cell membrane. In addition, it may be suggested that the intracellular ROS levels are responsible for the oxidative stress and the consequent cell death.

Author contribution

All authors contributed equally to this work. Ana Paula Dias Ribeiro, Flávia Zardo Trindade and Natália Mayumi Inada performed experiments and analysed data. Ana Cláudia Pavarina, Vanderlei Salvador Bagnato and Carlos Alberto de Souza Costa supervised the project, analysed and interpreted the data, and corrected the manuscript. Ana Paula Dias Ribeiro wrote the manuscript. All authors discussed the results and implications, and commented on the manuscript at all stages.

Acknowledgements

We would like to acknowledge the Center of Study in Optics and Photonics (CEPOF) at the Physics Institute of São Carlos (IFSC) of the University de São Paulo (USP) for developing the LED prototype specifically for this study. We also would like to acknowledge Professor Anibal Eugenio Vercesi from Medical Science School of the University of Campinas (UNICAMP) for helping with flow cytometry analysis

Funding

This work was partially supported by Fundação de Amparo à Pesquisa do Estado de São Paulo (FAPESP) [grant number 2007/04376-4].

References

- Ahn WS, Bae SM, Huh SW, Lee JM, Namkoong SE, Han SJ, et al. Necrosis-like death with plasma membrane damage against cervical cancer cells by photodynamic therapy. *Int J Gynecol Cancer* 2004;14:475–82.
- Allison RR, Cuenca RE, Downie GH, Camnitz P, Brodish B, Sibata CH. Clinical photodynamic therapy of head and neck cancers—a review of applications and outcomes. *Photodiagn Photodyn Ther* 2005;2:205–22.
- Allison RR, Bagnato VS, Cuenca R, Downie GH, Sibata CH. The future of photodynamic therapy in oncology. *Future Oncol* 2006;2:53–71.
- Aranha AMF, Souza PPC, Giro EMA, Hebling J, Costa CAS. Effect of curing regime on the cytotoxicity of resin-modified glass-ionomer cements applied to an odontoblast-cell line. *Dent Mater* 2006;22:864–9.
- Bertoloni G, Reddi E, Gatta M, Burlini C, Jori G. Factors influencing the haematoporphyrin-sensitized photoinactivation of *Candida albicans*. *J Gen Microbiol* 1989;135:957–66.
- Bliss JM, Bigelow CE, Foster TH, Haidaris CG. Susceptibility of *Candida* species to photodynamic effects of Photofrin. *Antimicrob Agents Chemother* 2004;48:2000–6.
- Bouillaguet S, Owen B, Wataha JC, Campo MA, Lange N, Schrenzel J. Intracellular reactive oxygen species in monocytes generated by photosensitive chromophores activated with blue light. *Dent Mater* 2008;24:1070–6.
- Buytaert E, Dewaele M, Agostinis P. Molecular effectors of multiple cell death pathways initiated by photodynamic therapy. *Biochim Biophys Acta* 2007;1776:86–107.
- Chandra J, Mukherjee PK, Leidich SD, Faddoul FF, Hoyer LL, Douglas LJ, Ghannoum MA. Antifungal resistance of candidal biofilms formed on denture acrylic in vitro. *J Dent Res* 2001;80:903–8.
- Chiu LL, Sun CH, Yeh AT, Torkian B, Karamzadeh A, Tromberg B, et al. Photodynamic therapy on keloid fibroblasts in tissue-engineered keratinocyte-fibroblast co-culture. *Lasers Surg Med* 2005;37:231–44.
- Demidova TN, Hamblin MR. Effect of cell-photosensitizer binding and cell density on microbial photoinactivation. *Antimicrob Agents Chemother* 2005;49:2329–35.
- de Souza Costa CA, Duarte PT, de Souza PP, Giro EM, Hebling J. Cytotoxic effects and pulpal response caused by a mineral trioxide aggregate formulation and calcium hydroxide. *Am J Dent* 2008;21:255–61.
- Donnelly RF, McCarron PA, Tunney MM, Woolfson A. Potential of photodynamic therapy in treatment of fungal infections of the mouth. Design and characterisation of a mucoadhesive patch containing toluidine blue O. *J Photochem Photobiol B* 2007;86:59–69.
- Donnelly RF, McCarron PA, Tunney MM. Antifungal photodynamic therapy. *Microbiol Res* 2008;163:1–12.
- Hanks CT, Sun ZL, Fang DN, Edwards CA, Wataha JC, Ritchie HH, Butler WT. Cloned 3T6 cell line from CD-1 mouse fetal molar dental papillae. *Connect Tissue Res* 1998;37:233–49.
- Hsieh YJ, Wu CC, Chang CJ, Yu JS. Subcellular localization of Photofrin determines the death phenotype of human epidermoid carcinoma A431 cells triggered by photodynamic therapy: when plasma membranes are the main targets. *J Cell Physiol* 2003;194:363–75.
- Jorge JH, Giampaolo ET, Vergani CE, Machado AL, Pavarina AC, Carlos IZ. Biocompatibility of denture base acrylic resins evaluated in culture of L929 fibroblasts. Effect of polymerisation cycle and post-polymerisation treatments. *Gerodontology* 2007;24:52–7.
- Karu TI. Effects of visible radiation on cultured cells. *Photochem Photobiol* 1990;52:1089–98.
- Konopka K, Goslinski T. Photodynamic Therapy in Dentistry. *J Dent Res* 2007;86:694–707.
- Lambrechts SAG, Aalders MCG, Van Marle J. Mechanistic study of the photodynamic inactivation of *Candida albicans* by cationic porphyrin. *Antimicrob Agents Chemother* 2005a;49:2026–34.
- Lambrechts SA, Schwartz KR, Aalders MC, Dankert JB. Photodynamic inactivation of fibroblasts by a cationic porphyrin. *Lasers Med Sci* 2005b;20:62–7.
- Lockwood DB, Wataha JC, Lewis JB, Tseng WY, Messer RL, Hsu SD. Blue light generates reactive oxygen species (ROS) differentially in tumor vs. normal epithelial cells. *Dent Mater* 2005;21:683–8.
- Maisch T, Bosl C, Szeimies RM, Lehn N, Abels C. Photodynamic effects of novel XF porphyrin derivatives on prokaryotic and eukaryotic cells. *Antimicrob Agents Chemother* 2005;49:1542–52.
- Mosmann T. Rapid colorimetric assay for cellular growth and survival: application to proliferation and cytotoxicity assays. *J Immunol Methods* 1983;65:55–63.
- Nikawa H, Jin C, Makihira S, Egusa H, Hamada T, Kumagai H. Biofilm formation of *Candida albicans* on the surfaces of deteriorated soft denture lining materials caused by denture cleansers in vitro. *J Oral Rehabil* 2003;30:243–50.
- Postigo F, Sagristá ML, De Madariaga MA, Nonell S, Mora M. Photosensitization of skin fibroblasts and HeLa cells by three chlorin derivatives: role of chemical structure and delivery vehicle. *Biochim Biophys Acta* 2006;1758:583–96.
- Serrano MC, Pagani R, Peña J, Portolés MT. Transitory oxidative stress in L929 fibroblasts cultured on poly(epsilon-caprolactone) films. *Biomaterials* 2005;26:5827–34.
- Taoufik K, Mavrogonatou E, Eliades T, Papagiannoulis L, Eliades G, Kletsas D. Effect of blue light on the proliferation of human gingival fibroblasts. *Dent Mater* 2008;24:895–900.
- Teichert MC, Jones MD, Usacheva MN, Biel MA. Treatment of oral candidiasis with methylene blue-mediated photodynamic therapy in an immunodeficient murine model. *Oral Surg Oral Med Oral Pathol Oral Radiol Endod* 2002;93:155–60.
- Wainwright M. Photodynamic antimicrobial chemotherapy (PACT). *J Antimicrob Chemother* 1998;42:13–28.

- Wataha JC, Lewis JB, Lockwood PE, Hsu S, Messer RL, Rueggeberg FA, Bouillaguet S. Blue light differentially modulates cell survival and growth. *J Dent Res* 2004;83:104–8.
- Williams JA, Pearson GJ, Colles MJ. Antibacterial action of photoactivated disinfection (PAD) used on endodontic bacteria in planktonic suspension and in artificial and human root canals. *J Dent* 2006;34:363–71.
- Wilson M, Mia N. Sensitisation of *Candida albicans* to killing by low-power laser light. *J Oral Pathol Med* 1993;22:354–57.
- Yu CH, Chen HM, Hung HY, Cheng SJ, Tsai T, Chiang CP. Photodynamic Therapy outcome for oral verrucous hyperplasia depends on the clinical appearance, size, color, epithelial dysplasia, and surface keratin thickness of the lesion. *Oral Oncol*. 2008;44:595–600.
- Zeina B, Greenman J, Purcell WM, Das B. Killing of cutaneous microbial species by photodynamic therapy. *Br J Dermatol* 2001;144:274–78.
- Zeina B, Greenman J, Corry D, Purcell WM. Cytotoxic effects of antimicrobial photodynamic therapy on keratinocytes in vitro. *Br J Dermatol* 2002;146:568–73.
- Zeina B, Greenman J, Corry D, Purcell WM. Antimicrobial photodynamic therapy: assessment of genotoxic effects on keratinocytes in vitro. *Br J Dermatol* 2003;148:229–32.

Received 29 June 2009/23 October 2009; accepted 6 November 2009

Published as Immediate Publication 6 November 2009, doi 10.1042/CBI20090032